2012

Direct exfoliation of graphite with a porphyrin - Creating functionalizable nanographene hybrids

Jenny Malig
ICMM

Adam W. I Stephenson
University of Wollongong

Pawel Wagner
University of Wollongong, pawel@uow.edu.au

Gordon G. Wallace
University of Wollongong, gwallace@uow.edu.au

David L. Officer
University of Wollongong, davido@uow.edu.au

See next page for additional authors

Direct exfoliation of graphite with a porphyrin - Creating functionalizable nanographene hybrids

Abstract

Exfoliation of graphite was achieved using a free-base porphyrin 1 resulting in an efficient fabrication of single-layer nanographene (NG)-1 hybrid platelets that can be further functionalized with other nanomaterials. The novel nanographene-porphyrin hybrids reveal efficient charge transfer in the excited state.

Keywords

porphyrin, graphite, functionalizable, exfoliation, direct, hybrids, creating, nanographene

Disciplines

Life Sciences | Physical Sciences and Mathematics | Social and Behavioral Sciences

Publication Details

Malig, J., Stephenson, A. W. I., Wagner, P., Wallace, G. G., Officer, D. L., Guldi, D. M. (2012). Direct exfoliation of graphite with a porphyrin - Creating functionalizable nanographene hybrids. Chemical Communications, 48 (70), 8745-8747.

Authors

Jenny Malig, Adam W. I Stephenson, Pawel Wagner, Gordon G. Wallace, David L. Officer, and Dirk M. Guldi

ChemComm

Chemical Communications

www.rsc.org/chemcomm

Volume 48 | Number 70 | 11 September 2012 | Pages 8717–8848

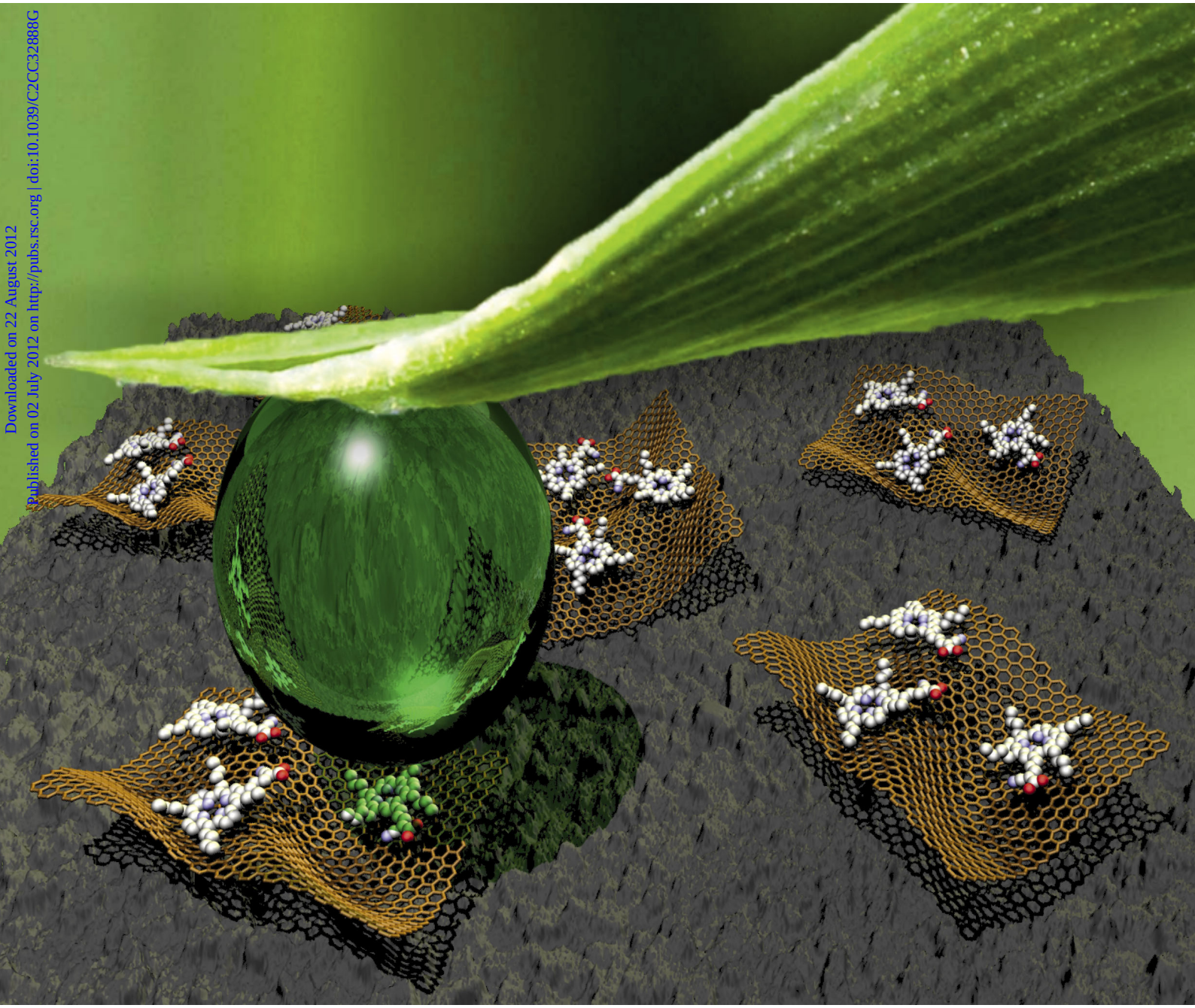

ISSN 1359-7345

RSC Publishing

COMMUNICATION

Dirk M. Guldi *et al.*

Direct exfoliation of graphite with a porphyrin – creating functionalizable nanographene hybrids

1359-7345(2012)48:70;1-#

ChemComm

Dynamic Article Links
View Online

Cite this: *Chem. Commun.*, 2012, **48**, 8745–8747

www.rsc.org/chemcomm

COMMUNICATION

Direct exfoliation of graphite with a porphyrin – creating functionalizable nanographene hybrids†

Jenny Malig,[a] Adam W. I. Stephenson,[b] Pawel Wagner,[b] Gordon G. Wallace,[b] David L. Officer[b] and Dirk M. Guldi*[ab]

Received 23rd April 2012, Accepted 14th June 2012
DOI: 10.1039/c2cc32888g

Exfoliation of graphite was achieved using a free-base porphyrin 1 resulting in an efficient fabrication of single-layer nanographene (NG)–1 hybrid platelets that can be further functionalized with other nanomaterials. The novel nanographene–porphyrin hybrids reveal efficient charge transfer in the excited state.

En route towards graphene a number of versatile approaches have recently been established. Particularly promising is the direct growth of graphene by means of silicon removal from SiC[1] and chemical vapor deposition (CVD) on Cu[2] substrates. No doubt, this growth approach offers full control over high quality graphene. A major drawback is, nevertheless, the strong substrate graphene interactions. On the contrary, a full-fledged chemical bottom-up approach, that is, the step-by-step synthesis of molecular building blocks leading to graphene like structures (*i.e.*, nanoribbons, *etc.*) is based on the pioneering work by Muellen *et al.*[3] Finally, a wet chemical approach should be considered, in which ultrasound treatment of graphite leads to high quality/high yield exfoliation.[4] A particular benefit of this wet chemical approach is that the resulting graphene is stabilized in organic solvents and also in water in the presence of surface active surfactants.[5] To this end, we and other have recently probed the exfoliation of graphite in liquid (*i.e.*, organic solvents and water).[5b,6] In particular, photo- and redoxactive building blocks such as phthalocyanines or porphyrins were directly immobilized onto the basal plane of graphene or electrostatically bound to a charged exfoliation agent. In the resulting hybrids, which comprised of, however, few layers rather than single layer graphene, photoinduced electron transfer reactions afforded metastable charge transfer states. Here, we wish to report on a novel multifunctional free base porphyrin (**1**), which guarantees to exfoliate graphite to yield single to few layer graphene/nanographene (NG), to non-covalently functionalize/dope graphene, to power an intrahybrid electron transfer (Scheme 1), and, to immobilize photoactive nanoparticles like TiO_2.

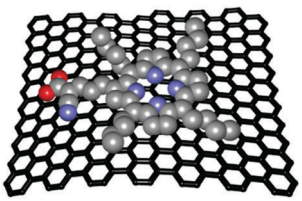

Scheme 1 Representation of a nanographene (NG)–porphyrin **1** hybrid.

The synthesis of the required tetraalkylporphyrin **1** presented us with the opportunity to develop a new general synthesis of this type of porphyrin as shown in Scheme S1 (ESI†), analogous to what we have developed for tetraarylporphyrin DSSC dyes.[7,8] Key features of this synthesis include the improvement of the previously reported low yielding Vilsmeier formylation of tetraalkylporphyrins[9] by using a 100 times excess of the Vilsmeier reagent incorporating *N*-methylformanilide instead of DMF at 60 °C, and employing a milder porphyrin demetalation previously described by Ponomarev and Maravin.[10] Porphyrin allylaldehyde **4** (Scheme S1, ESI†) could then be obtained in high yield (80%) following purification by a modified procedure of Ishkov *et al.*,[11] in which the deprotection and isomerization steps were performed on the crude Wittig reaction mixture. Knoevenagel condensations of **4** with cyanoacetic acid gave excellent yields of the free base porphyrin **1**.

In order to probe the interaction of the porphyrin with graphene, the ground state features of porphyrin **1** were initially investigated by steady-state absorption spectroscopy and electrochemical measurements. As has previously been observed in the absorption spectrum for this type of porphyrin with extended conjugation, the characteristic Soret band, which maximizes at 425 nm, is asymmetric and strongly broadened (Fig. 1). The latter is a result of both the β-pyrrolic substitution by the conjugated linker that causes a loss in symmetry as well as some aggregation effects. Evidence for the aggregation effect is discernable in the spectra of a series of dilutions, which were performed in a concentration regime between 1.88×10^{-6} and 1.43×10^{-6} M. They feature an isosbestic point at 437 nm and an increase in symmetry (Fig. 1). In addition, the Q-bands shift hypsochromically upon dilution to 530, 581, 616, and 677 nm.

[a] *Department of Chemistry and Pharmacy & Interdisciplinary Center for Molecular Materials (ICMM), Friedrich-Alexander-Universität Erlangen-Nürnberg, 91058 Erlangen, Germany. E-mail: guldi@chemie.uni-erlangen.de; Fax: +49 9131 8527341; Tel: +49 9131 8527340*
[b] *ARC Centre of Excellence for Electromaterials Science and the Intelligent Polymer Research Institute, University of Wollongong, NSW 2522, Australia. E-mail: davido@uow.edu.au; Fax: +61 2 4221 3114; Tel: +61 2 4221 3127*
† Electronic supplementary information (ESI) available. See DOI: 10.1039/c2cc32888g

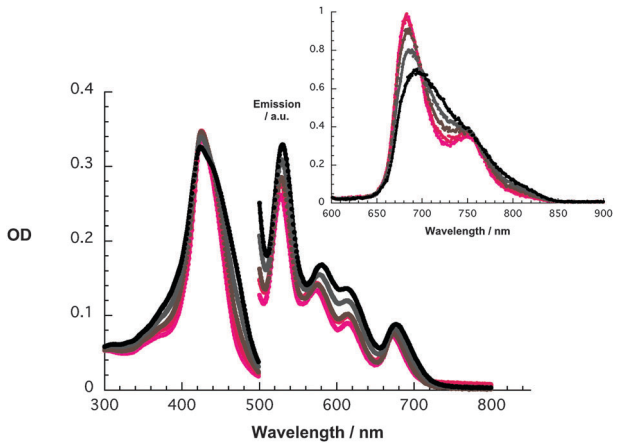

Fig. 1 Upper part: absorption spectra of **1** in THF with concentrations ranging from 1.88×10^{-6} (black) to 1.43×10^{-6} M (pink) – the 500 to 800 nm range has been amplified by a factor of 7. Inset shows the corresponding fluorescence spectra upon excitation at 515 nm.

From the long wavelength absorption seen in Fig. 1, we have derived the energy of the first singlet excited state as 1.8 eV.

The excited state characteristics were determined by fluorescence spectroscopy. As Fig. 1 documents, upon exciting **1** at 515 nm, a surprisingly broad fluorescence band centered at 703 nm was registered. However, in line with the absorption measurements – *vide supra* – upon dilution the rather broad fluorescence centered at 703 nm was displaced by a set of two fluorescence peaks with maxima at 686 and 750 nm (Fig. 1). Notably, the latter pattern resembles the typical fluorescence spectra of monomeric porphyrins and a fluorescence quantum yield of 0.05. A marked Stokes shift of 590 cm^{-1} in concentrated solutions results from the difference between the long wavelength absorption and the short wavelength fluorescence for the aggregated species. A Stokes shift of 280 cm^{-1} for the diluted solution supports the notion of aggregation phenomena (Fig. 1).

Corroborating results came from time-correlated single photon-counting (TCSPC) experiments. Exciting **1** at 403 nm results in fluorescence features at 686 and 750 nm, which were best fit by two-exponential fitting functions (Fig. S2, ESI†). Analyses of the 686 nm feature – relating to the less aggregated/monomeric form of **1** – reveal lifetimes of 3.0 and 7.9 ns with a relative distribution of 38 and 62%. The 750 nm feature – correlating with the more aggregated form of **1** – is analyzed with 2.6 and 7.4 ns lifetimes and a relative distribution of 63 and 37%.

As a second step, femtosecond transient-absorption measurements were performed with **1** in THF using 387 nm and 150 fs excitation pulses. Ground-state bleaching is observed in Fig. S3 (ESI†) across the visible region with local minima at 455, 534, 587, 616, and 700 nm. In addition, we note transient maxima at 509, 560, 645, 745, 860, and 1080 nm, which are attributed to the singlet excited state features of **1**. These singlet excited features convert *via* a very rapid intersystem crossing (*i.e.*, 8.5×10^{8} s^{-1}) to the energetically lower-lying triplet excited features. The most prominent feature of the corresponding triplet excited state characteristics is the 890 nm maximum.

Having determined the key characteristics of **1**[12] that would enable tracking its successful immobilization onto the basal plane of graphene, a THF solution of **1** (10^{-6} M) was ultrasonicated for 30 minutes with natural graphite. Such a treatment resulted in the direct exfoliation of graphite and the concomitant immobilization of **1** onto graphene. The immobilization of **1** was followed by emission spectroscopy. Here, the quantitative quenching of the porphyrin fluorescence affirms the successful integration (Fig. S6, ESI†). Following 10 000 *g* centrifugation for 30 minutes in order to remove the remaining graphite, the supernatant was utilized for further characterization – see ESI.† Taking the absorption at 660 nm into consideration typical nanographene concentrations were in the range of 0.1 mg ml^{-1}.[5] These stock solutions were, however, diluted prior to any in-depth characterization. The corresponding dispersions are stable over months and obey the Lambert–Beer Law as shown in Fig. S4 (ESI†) and should be considered as real solutions of extraordinary stability. Such solutions (*i.e.*, nanographene–**1**) give rise to an absorption maximum at 265 nm.

Raman spectroscopy confirms the successful exfoliation of graphite into single to few layer graphene/nanographene (NG), Fig. 2 and Fig. S5 (ESI†). Of particular importance is the strong D-band centered at 1342 cm^{-1}. Fig. S5 (ESI†) documents that the latter is absent in the several hundred micrometers thick flakes of natural graphite and is assigned to the smaller flake sizes upon exfoliation into nanographene (NG). As a matter of fact, contributions from the edges to the double resonant Raman effect increase upon reducing the lateral dimension. The latter is likely to happen during graphite exfoliation by ultrasound treatment. The confinement is further affirmed by the symmetric 2D-band, with a 2D/G ratio of *ca.* 0.9 and a full width of half magnitude (FWHM) of 53 cm^{-1} when fit by a single Lorentzian (Fig. 2). At this point we conclude that the morphology is best described as wrinkled and intertwined sheets – *vide infra*. The Bernal stacks as present in graphite were displaced by ultrasound treatment resulting in exfoliated graphite. Self-aggregation and partial re-aggregation of one or several graphene sheets resulted in an intrinsic turbostratic structure.[13]

The strong electronic interactions between NG and **1** are even more evident in fluorescence experiments. Here, the complete quenching of the fluorescence of **1**, when exciting NG–**1** either in the Soret- or in the Q-band regions, is observed (Fig. S6, ESI†) with fluorescence lifetimes that are masked by the temporal resolution of our instrument. In fact, this finding indicates a recombination pathway other than emission and

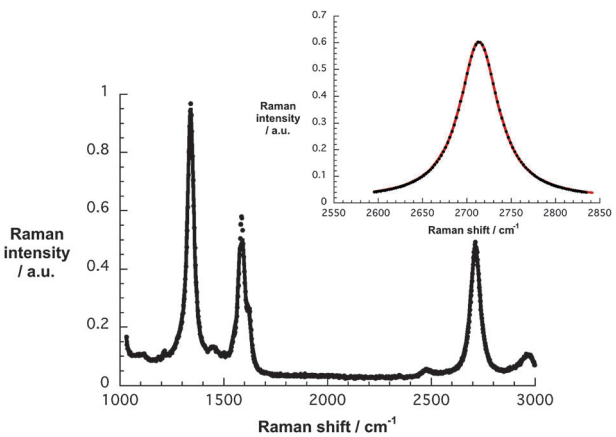

Fig. 2 Raman spectrum of NG–**1** dispersion in THF drop-cast onto a silicon oxide wafer and excited at 532 nm. Inset shows the single Lorentzian fit (red) of the 2D-band (black).

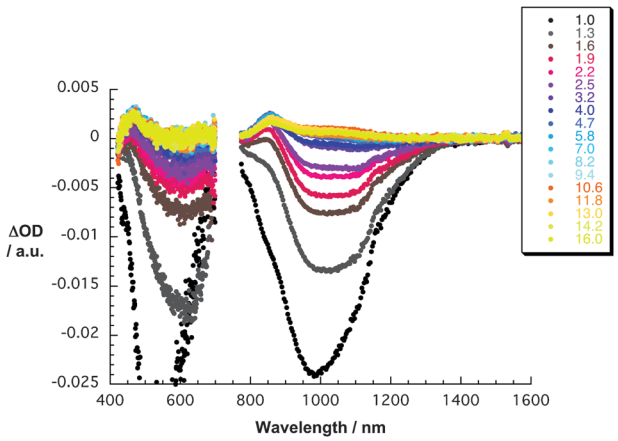

Fig. 3 Differential absorption spectra (visible) obtained upon femtosecond pump probe experiments (387 nm) of NG–**1** in THF with several time delays between 1.0 and 16.0 ps at room temperature.

hints to electron or energy transfer deactivation of photoexcited **1**. Additional resonant Raman experiments were performed with 633 nm excitation (Fig. S7, ESI†). Resonant excitation of **1** at 633 nm superimposes, however, the entire Raman spectrum by strong emission and hampers the identification of Raman peaks. A comparison with the non-resonant Raman spectrum (Fig. S8, ESI†), generated by 1064 nm excitation, assists in assigning the Raman bands. Peaks, which appear in the range from 1100 to 1580 cm^{-1} and which are superimposed with the D- and G-bands at 1101 ($\delta(C_\beta–H)$), 1125, 1195, 1224 ($\nu(C_\alpha–N)$), 1301, 1454, 1466 ($\nu(C_\alpha–C_\beta)$ + $\delta(C_\beta–H)$), 1488, 1513, 1530, 1557 (($\nu(C_\alpha–C_m)$), and 1574 cm^{-1} relate to porphyrin centered modes.[14] Atomic force microscopy sheds light onto the flake height and size distribution – Fig. S9 (ESI†). The graphene flakes were about 5 nm in height owing to the presence of strongly folded and intertwined sheets – *vide supra*. The lateral sizes are found to be up to 500 nm. Self-aggregation, re-aggregation, and rolling up of graphene sheets, as implied from Raman investigations, should be considered in the interpretation of the AFM height profiles – Fig. S10 (ESI†). Transmission electron microscopy further supports this notion – sheets are discernable that feature surface wrinkles and lateral dimensions of 1000 nm – Fig. S11 (ESI†).

To gain deeper insights into the interactions, we performed transient absorption experiments with NG–**1**. Fig. 3 testifies that the singlet excited characteristics of **1** evolve despite the presence of NG upon 387 nm photoexcitation of NG–**1**. This confirms the successful excitation of **1** – *vide supra*. Simultaneously with the rapid singlet excited state decay (5 ps) the formation of a new transient species evolves in the 400 to 800 nm range with distinct maxima at 465 nm as well as minima at 620 nm. Of key importance is the resemblance of these attributes with those of the one-electron oxidized radical cation of **1**, as they were determined in pulse radiolytic investigations.[12] Similarly, the 800 to 1600 nm range is important, which immediately after the photoexcitation is dominated by phonon related bleaching.[6] Here, new features were noted during the transient decay (5 ps), namely maxima at 860 and 1075 nm. Importantly, the 860 nm maximum is attributed to the radical cation of **1** formed upon photoexcitation. Taking the aforementioned into consideration, we imply a rapid charge transfer, that is, an oxidized porphyrin and new conduction band electrons in NG. Multi-wavelength analyses of the newly developed charge transfer state reveal its metastability with a lifetime of 265 ps – Fig. S12 (ESI†).

In preliminary assays we have exposed NG–**1** to suspensions of TiO_2 nanoparticles. TEM images as shown in Fig. S10 (ESI†) reveal that the presence of TiO_2 nanoparticles is restricted exclusively to areas covered with NG–**1**.

In contrast to our recent work, the current work demonstrates the versatility of porphyrins to realize novel NG hybrids for photoconversion. In particular, porphyrin **1** is key towards the successful exfoliation of graphite to yield stable suspensions of single and few layer graphene/nanographene (NG). In addition, chemical doping by shifting electron density from porphyrin **1** to NG is a consequence of mutually interacting constituents and, in turn, dominates the ground and excited state characteristics. In fact, the latter is the inception to the formation of a metastable charge transfer state.

Notes and references

1 (*a*) K. V. Emtsev, A. Bostwick, K. Horn, J. Jobst, G. L. Kellogg, L. Ley, J. L. McChesney, T. Ohta, S. A. Reshanov, J. Rohrl, E. Rotenberg, A. K. Schmid, D. Waldmann, H. B. Weber and T. Seyller, *Nat. Mater.*, 2009, **8**, 203; (*b*) C. Berger, Z. Song, T. Li, X. Li, A. Y. Ogbazghi, R. Feng, Z. Dai, A. N. Marchenkov, E. H. Conrad, P. N. First and W. A. de Heer, *J. Phys. Chem. B*, 2004, **108**, 19912.

2 (*a*) S. Bae, H. Kim, Y. Lee, X. Xu, J.-S. Park, Y. Zheng, J. Balakrishnan, T. Lei, H. R. Kim, Y. I. Song, Y.-J. Kim, K. S. Kim, B. Ozyilmaz, J.-H. Ahn, B. H. Hong and S. Iijima, *Nat. Nanotechnol.*, 2010, **5**, 574; (*b*) Z. Sun, Z. Yan, J. Yao, E. Beitler, Y. Zhu and J. M. Tour, *Nature*, 2010, **468**, 549.

3 (*a*) M. D. Watson, A. Fechtenkotter and K. Muellen, *Chem. Rev.*, 2001, **101**, 1267; (*b*) B. Schmaltz, T. Weil and K. Muellen, *Adv. Mater.*, 2009, **21**, 1067.

4 Y. Hernandez, V. Nicolosi, M. Lotya, F. M. Blighe, Z. Sun, S. De, I. T. McGovern, B. Holland, M. Byrne, Y. K. GunKo, J. J. Boland, P. Niraj, G. Duesberg, S. Krishnamurthy, R. Goodhue, J. Hutchison, V. Scardaci, A. C. Ferrari and J. N. Coleman, *Nat. Nanotechnol.*, 2008, **3**, 563.

5 (*a*) M. Lotya, Y. Hernandez, P. J. King, R. J. Smith, V. Nicollosi, L. S. Karlsson, F. M. Blighe, S. De, Z. Wang, I. T. McGovern, G. S. Duesberg and J. N. Coleman, *J. Am. Chem. Soc.*, 2009, **131**, 3611; (*b*) J. Geng, B.-S. Kong, S. B. Yang and H.-T. Jung, *Chem. Commun.*, 2010, 5091.

6 (*a*) J. Malig, N. Jux, D. Kiessling, J.-J. Cid, P. Vázquez, T. Torres and D. M. Guldi, *Angew. Chem., Int. Ed.*, 2011, **50**, 3561; (*b*) J. Malig, C. Romero-Nieto, N. Jux and D. M. Guldi, *Adv. Mater.*, 2012, **24**, 799; (*c*) G. Katsukis, J. Malig, C. Schulz-Drost, S. Leubner, N. Jux and D. M. Guldi, *ACS Nano*, 2012, **6**, 1915.

7 Q. Wang, W. M. Campbell, E. E. Bonfantani, K. W. Jolley, D. L. Officer, P. J. Walsh, K. Gordon, R. Humphry-Baker, M. K. Nazeeruddin and M. Graetzel, *J. Phys. Chem. B*, 2005, **109**, 15397.

8 K. W. Jolley, D. L. Officer, W. M. Campbell, P. Wagner, L. Schmidt-Mende, Q. Wang, R. Humphry-Baker, M. K. Nazeeruddin and M. Grätzel, *J. Phys. Chem. C*, 2007, **111**, 11760.

9 (*a*) M. O. Senge, V. Gerstung, K. Ruhlandt-Senge, S. Runge and I. Lehmann, *J. Chem. Soc., Dalton Trans.*, 1998, 4187; (*b*) T. Yamamura, S. Suzuki, T. Taguchi, A. Onoda, T. Kamachi and I. Okura, *J. Am. Chem. Soc.*, 2009, **131**, 11719.

10 G. V. Ponomarev and G. B. Maravin, *Khim. Geterotsikl. Soedin.*, 1982, **1**, 59.

11 Y. V. Ishkov, Z. I. Khilina, Zh. V. Grushevaya and A. M. Shul'ga, *Zh. Org. Khim.*, 1993, **29**, 2270.

12 The electrochemical features of **1** are typical of a tetrasubstituted porphyrin with two reversible reductions at potentials of −1.4 and −1.6 V as well as quasi-reversible oxidation potentials of +0.8 and +1.3 V.

13 A. A. Green and M. C. Hersam, *Nano Lett.*, 2009, **9**, 4031.

14 T. M. Cotton, S. G. Schultz and R. P. Van Duyne, *J. Am. Chem. Soc.*, 1982, **104**, 6528.